


Article

Electrochromic Properties of the Vanadium Pentoxide Doped with Nickel as an Ionic Storage Layer

Tien-Chai Lin ¹, Bai-Jhong Jheng ² and Wen-Chang Huang ^{1,3,*} 

¹ Department of Electrical Engineering, Kun Shan University, Yongkang Dist., Tainan 710303, Taiwan; tienchai@mail.ksu.edu.tw

² Tintable Kibing Cooperation, Rende Dist., Tainan 71758, Taiwan; chris81809@gmail.com

³ Green Energy Technology Research Center, Kun Shan University, Yongkang Dist., Tainan 710303, Taiwan

* Correspondence: wchuang@mail.ksu.edu.tw

Abstract: The electrochromic property of nickel doped vanadium pentoxide (V_2O_5) deposited by a co-sputtering system is investigated. The structural analysis of the thin film was done by an X-ray diffraction (XRD) analyzer. The surface morphology of the film was studied by a field emission scanning electron microscopy (FE-SEM). The composition of the film was detected by an Auger analysis. The electrochromic properties of the device were measured by cyclic voltammetry. For the undoped V_2O_5 thin film, the charge storage capacity increases with the thickness and is 42.58 mC/cm^2 at the thickness of 192.4 nm after 2 h deposition. For the Ni-doped V_2O_5 , the Ni-V-O film shows V_2O_5 structural dominate with cathode coloration in the lower Ni deposition power region and the charge storage capacity decreases with the increases of the power, while the Ni-V-O film transfers to NiO structural dominate with anodic coloration at the realm of higher Ni doping. The charge storage capacity increases with the increase of Ni doping. It can reach to 101.35 mC/cm^2 . The Ni-V-O electrochromic film shows improvement of transmittance difference between colored and bleached values and improvement of charge store capacity as it is compared to pure V_2O_5 films.

Keywords: electrochromic; vanadium pentoxide; nickel; ionic storage layer



Citation: Lin, T.-C.; Jheng, B.-J.;

Huang, W.-C. Electrochromic Properties of the Vanadium Pentoxide Doped with Nickel as an Ionic Storage Layer. *Energies* **2021**, *14*, 2065. <https://doi.org/10.3390/en14082065>

Received: 11 February 2021

Accepted: 6 April 2021

Published: 8 April 2021

Publisher's Note: MDPI stays neutral with regard to jurisdictional claims in published maps and institutional affiliations.



Copyright: © 2021 by the authors. Licensee MDPI, Basel, Switzerland. This article is an open access article distributed under the terms and conditions of the Creative Commons Attribution (CC BY) license (<https://creativecommons.org/licenses/by/4.0/>).

1. Introduction

Electrochromic materials become important due to the variation of transmittance of visible light under the application of an external stimulus [1,2]. The materials exhibit a reversible change of their color through charge transfer. One of the important classes of electrochromic material is electrochromic oxide [3]. The electrochromic oxide materials can be divided into two different kinds of material, cathodic coloration material and anodic coloration material. The oxides of Ti, Nb, Mo, Ta, and W belong to cathodic coloration materials and the oxides of Cr, Mn, Fe, Co, Ni, Rh, and Ir belong to the anodic coloration materials. There are some electrochromic oxide materials that both show the cathodic and anodic coloration, such as vanadium pentoxide (V_2O_5) [4].

Due to the redox property of the V_2O_5 thin film, the film is a suitable material for the application of lithium ion battery, gas sensor and electrochemical devices. V_2O_5 thin film shows electrochromic with its reversible changes of color between yellow and gray when an external stimulus voltage is applied [5]. This is because it possesses a stacked laminate structure which makes ion intercalation easier [6]. However, the electrochromic properties of a pure V_2O_5 are very limited due to its low conductivity and low electrochemical stability [7–9]. To overcome these problems, some studies have addressed the synthesis and fabrication of nanostructured V_2O_5 film so as to improve the electrochromic properties of the film [10]. However, the electrochromic device with nanostructure creates additional problems of reliability and stability.

The process of metal-doping of the electrochromic oxide shows high-performance and reliability has been proposed on tungsten trioxide (WO_3) and nickel oxide (NiO)

film [11,12]. The chromic mixed metal oxide films often show more natural colors than intrinsic ones in their coloring states. This is due to the improvement of the optical band gap by the metal-doping [13]. M.A. Ashrafi et al. presented the $(\text{MoO}_3)_{1-x}(\text{V}_2\text{O}_5)_x$ chromic mixed metal oxide films [14]. It is known that molybdenum oxide (MoO_3) can be a material of photochromic [15] and vanadium oxide is a popular thermochromic material [16]. As molybdenum oxide mixed with vanadium oxide in a single structure, this film may provide both photochromic and thermochromic effects, and also has an improvement in coloring performance. The vanadium pentoxide with niobium-doping [17] shows that the doped samples have better stability than the undoped vanadium pentoxide. In this study, we are interested to deposit a mixed metal oxide film, Ni-V-O, a combination of nickel oxide (NiO) with V_2O_5 in a single structure.

NiO is a material of low cost, has good cyclic reversibility, high coloring efficiency and good durability [18–20]. It shows a brownish color at the colored state and a high transparency at the bleached state [1,21]. If these two chromic oxide materials, NiO and V_2O_5 mixed together in the same electrochromic device, it is expected to improve the transparency modulation. The improvement of transparency modulation would make it practical for the applications of smart windows [22–24]. However, the electrochromic property of metal oxides with different crystal structures are not in direct proportion to the mixing-ratio of chromic oxide. Therefore, it is intriguing to study the variation of optical, electrochromic properties with the mixing ratio.

Some techniques that were used to deposit the electrochromic oxide films are as follows: sputtering [25], evaporation [26], sol-gel [27], chemical vapor deposition [26], spray pyrolysis [28], and pulsed laser deposition [13]. Sputtering is an efficient technique for deposition of thin films. By using sputtering, it can successfully deposit mixed oxides and have a good control of sputtering power toward targets, gas flow rate, deposition thickness, and the substrate heating temperature. These parameters provide good processes for the deposition of a variety chemical compositions. This paper addresses the deposition of mixed chromic V_2O_5 films by adding NiO by a co-sputtering technique. The structural, optical and electrochromic properties of the film are investigated.

2. Experiments

The ITO glass substrate with a resistivity of $6 \Omega\text{-cm}$ was first cleaned by using acetone, isopropanol and DI water in sequence to remove any surface contamination, and then dried with the dry nitrogen flow. The dimension of each sample is $4 \times 2 \text{ cm}^2$. The thin film was deposited by an RF magnetron co-sputtering equipped. Both a V_2O_5 ceramic target and a Ni target with their purity of 99.9% and 7.62 cm in diameter were used. Argon, oxygen, and nitrogen with purity of 99.99% were inlet to the chamber during the deposition process. The base pressure of the chamber was 5×10^{-5} Torr and the processing pressure was constant at 5 mTorr at the flow of pure argon working gas of 5 sccm. The substrate holder was not heated during deposition. For the V_2O_5 thin film, the RF power toward the V_2O_5 ceramic target was 120 W, the deposition time was 1, 2 and 3 h. For the Ni-V-O thin film, the nickel doping effect toward the V_2O_5 film is stressed. The RF power toward the V_2O_5 ceramic target was 120 W, the deposition time was 2 h, the ratio of Ar: O_2 flow was 10:1 and the power toward the Ni target was varied as 10, 20, 30, 50, and 80 W, respectively.

The phase formation of the film was detected by an X-ray diffraction (XRD) analyzer. The surface morphology of the film was evaluated by field emission scanning electron microscopy (FE-SEM). The composition of the film was detected by an Auger analysis. The transmittance of the films was measured by a UV-Vis. The electrochromic property of the films was evaluated by a cyclic voltammetry (CV) measurement. The setup of the CV measurement system was performed by using a potentiometer in a three-electrode cell where the work electrode, reference electrode and counter electrode was the Ni-V-O film, a silver wire, and a platinum foil, respectively. The electrolyte was a 0.1 mol/L lithium perchlorate (LiClO_4). The CV measurements were performed in a potential range from

−2.5 to +2.5 V with a speed of 10 mV/s. The chronoamperometry measurements were evaluated at a potentials range of −2.5 and +2.5 V at a period of 60 s.

The charge density (Q) of the films evaluated from the CV curve by the following relation [29]:

$$Q(\text{charge density}) = \frac{1}{\nu \cdot A} \int_{V_i}^{V_f} I(V) dV$$

where ν is the sweep rate, V_i is the initial sweep voltage, V_f is the final sweep voltage, A is the area of the sample, I is the current.

The coloration efficiency (CE) is defined as the change in optical density at a specific wavelength divided by the inserted charge density (Q), as expressed in the following equation:

$$CE(\lambda) = \ln[T_{bleach}/T_{color}] / Q \left(\text{cm}^2 / \text{C} \right)$$

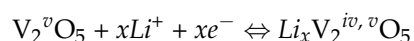
where, T_{bleach} is the transmittance of the film in the bleached state, T_{color} is the transmittance of the film in the colored state, and Q is the insert charge density. High coloration efficiency can provide a large optical modulation with low charge insertion or extraction and is a crucial parameter for practical electrochromic devices.

3. Results and Discussion

3.1. Electrochromic Property of V_2O_5 Thin Film

The V_2O_5 thin film property is dependent on the process conditions. The RF power toward the V_2O_5 ceramic target is kept at 120 W and the period time for deposition of the film is varied to observe its thickness effect toward electrochromic property. The thickness of the V_2O_5 film is 98.9, 192.4 and 288.2 nm with respect to the deposition time of 1, 2, and 3 h, respectively. As the thickness of the film is increased, the surface becomes rougher. This would give rise to more sites to accommodate the charges.

It is known that the color of the V_2O_5 thin film changes from yellow to gray [30]. Figure 1 shows the transmittance of the V_2O_5 film, the curve in black-square is the transmittance without bias. As the potential applies from −2.5 to 2.5 V, the sample transforms from gray to yellow with oxidation reaction as shown with a red line. As the potential applies from 2.5 to −2.5 V, the sample transforms from yellow to gray through reduction state as shown with a green line. In order to measure the transparency difference of oxidation/reduction of the film, the transparency difference is defined as $\Delta T = T_{oxidation} - T_{reduction}$ at the wavelength of 600 nm. The ΔT increased from 1.8 to 25.6% as the thickness of the film increases from 98.9 to 288.2 nm of the film. For the further discussion of the Ni doping effect, the V_2O_5 sample of 2 h deposition was chosen as shown in Figure 1. Its ΔT is 9.5% and its coloration efficiency of the V_2O_5 thin film is $2.04 \text{ cm}^2 / \text{C}$. The V_2O_5 sample shows low transmittance both on bleached and colored states and their transmittance is 60.0% and 50.5%, respectively. Ideally, the V_2O_5 film is yellow in oxidized state and it changes to gray that is reduced state as applying cathodic potential. While, our experimental sample shows dark gray in the colored state and light gray in the bleached state. The reaction is being described as the following [7,20]:



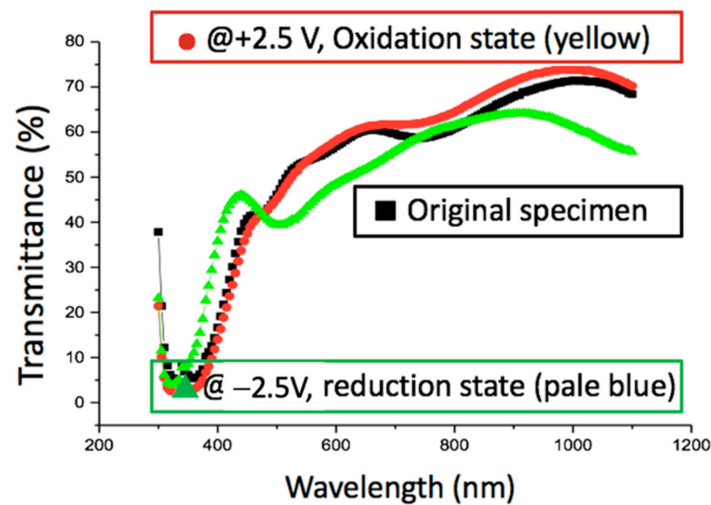


Figure 1. The transmittance of the V_2O_5 thin film; the original sample, colored sample and bleached sample are indicated by squares, circles and triangles, respectively.

CV measurement was used to study the effectiveness of the V_2O_5 thin films as ion storage layer of electrochromic devices, and the obtained results are displayed in Figure 2. The charge capacity is 29.18, 42.58 and 54.71 mC/cm^2 as the film thickness of V_2O_5 thin film is 98.9, 192.4 and 288.2 nm, respectively. The increase of the charge capacity is due to the increase of thickness and the roughness.

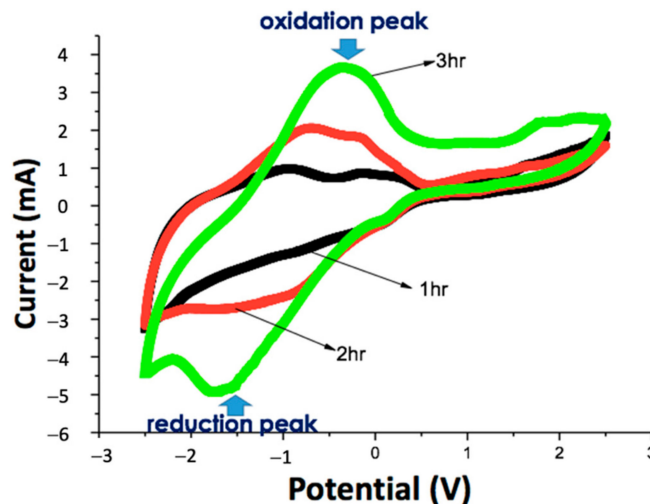


Figure 2. Cyclic voltammetry of the V_2O_5 thin films as ion storage layer of the electrochromic device.

3.2. Electrochromic Property of Ni-V-O Thin Film

It is reported [13] that chromic mixed metal oxide film has more natural colors than single chromic oxide material in their coloring states. This effectiveness is due to the improvement of the optical band gap. Nickel oxide (NiO) is a material of anodic coloration and it is transparent at the state of cathodic coloration. If the vanadium pentoxide was mixed with nickel oxide in a single structure, this new structure may provide a complementary electrochromic effect and improve coloring performance. The optical and electrochromic properties of the compositional variation between vanadium oxide and nickel oxide of the Ni-V-O film is stressed. Co-sputtering to the V_2O_5 ceramic target and to the Ni-metal target was through the sputtering gas, argon and oxygen to deposit the Ni-V-O chromic mixed-metal oxide film.

The thin film of mixed nickel oxide and vanadium pentoxide in a single structure was realized by co-deposition of Ni and V_2O_5 on a glass substrate. The compositions of the film

are summarized in Table 1. The thickness of the Ni-V-O mixed oxide thin film increased as the power toward the Ni target increased, it is 221 nm at the power of 10 W and is 337 nm as the power increases to 80 W. The atomic percentage of each element of the film was detected by an Auger analyzer. It shows the atomic percentage of Ni, V and O is 3.20, 26.04 and 70.76%, respectively at the sample of 10 W. The atomic percentage of Ni increases with the increase of the power. As the power reaches 50 W, the atomic percentages of Ni and V are comparable and they are 18.83 and 19.30%, respectively. As the power further increases to 80 W, the atomic percentage of Ni is more than two times of V. The atomic percentage of O shows a slight decrease as the power increases.

Table 1. The composition of the Ni-V-O mixed oxide film with respect to various sputtering powers toward the Ni target.

Power (W)	10	20	30	50	80
Thickness (nm)	221	241	259	282	337
Ni (at. %)	3.20	4.68	7.64	18.83	21.17
V (at. %)	26.04	24.52	29.97	19.30	11.47
O (at. %)	70.76	70.81	62.39	61.86	61.36

Figure 3 shows the XRD patterns of the Ni-V-O mixed oxide film with various sputtering powers toward the Ni target. There was no diffraction peak observed in the pattern and indicates the structure of Ni-V-O film is amorphous. As we mentioned above, the structure of the V_2O_5 film which we deposited is amorphous. Here, the co-sputtered Ni-V-O film is also amorphous. It means the addition of Ni into the V_2O_5 film does not change its amorphous structure.

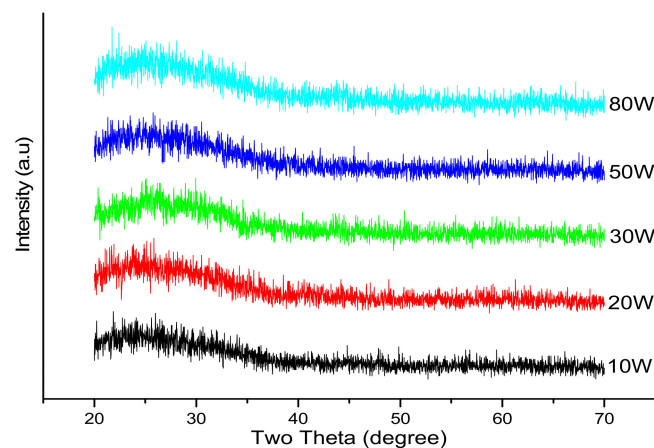


Figure 3. The XRD patterns of the Ni-V-O mixed oxide film with various sputtering powers toward the Ni target.

The morphology of the Ni-V-O film with magnitude of the pictures is $50,000\times$ with respect to the power that was observed by the FE-SEM as shown in Figure 4a–e. The surface shows small agglomerations at the sample of low power deposition. This is due to nonuniform doping of Ni at this low power deposition. The nonuniform doping effect is reduced as the power toward the Ni target increased. As the power increases to 50 W, the film shows regional gaps. These regional gaps disappear as the power further increases to 80 W. The atomic ratio of element Ni is larger than that of V, so the morphology of the Ni-V-O film is smooth and the gaps were filled.

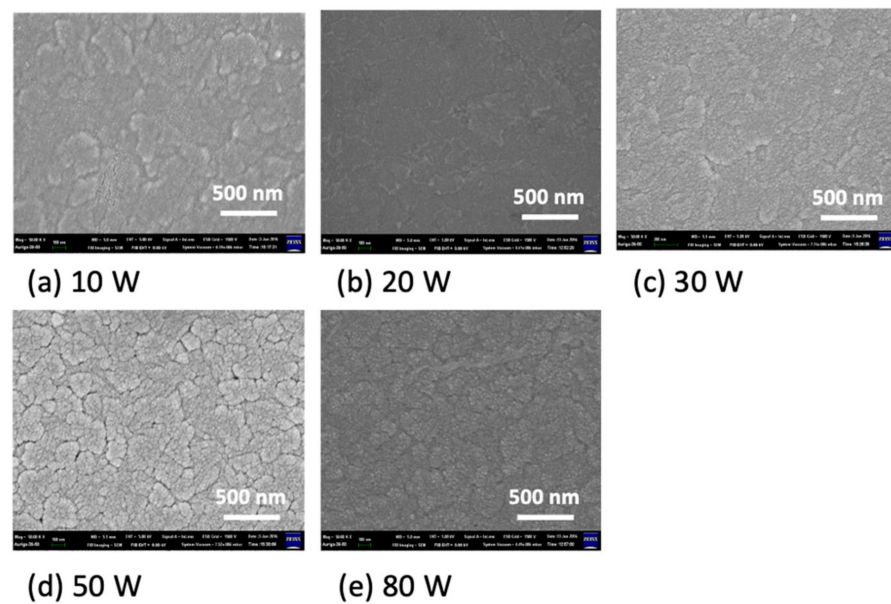


Figure 4. The surface morphology of the Ni-V-O film by FE-SEM with respect to different powers toward the Ni target (a) 10 W, (b) 20 W, (c) 30 W, (d) 50 W, and (e) 80 W, respectively.

The effectiveness of the Ni addition on the optical properties of the Ni-V-O films was evaluated in the range of 300–1100 nm, and the results are shown in Figure 5a–e. There are three curves in each figure, they are original specimen (without bias), oxidation state (potential at +2.5 V), and reduction state (potential at −2.5 V), and they are shown on the curves as a black square, red circle and green triangle, respectively. The difference of transparency is defined as $\Delta T = T_{\text{oxidation}} - T_{\text{reduction}}$ at the incident wavelength of 600 nm. Table 2 shows the summary of ΔT of the Ni-V-O samples with respect to various powers.

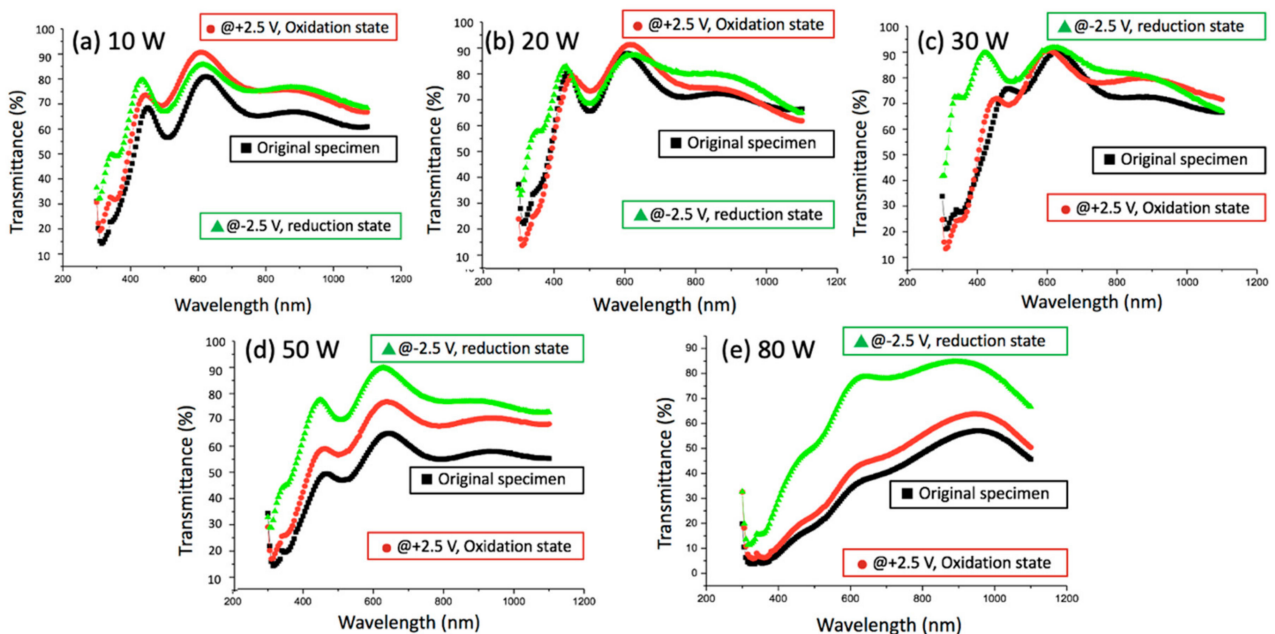


Figure 5. The transmittance of the Ni-V-O thin film, the original sample (square), colored sample (circle) and bleached (triangle) sample (a) 10, (b) 20, (c) 30, (d) 50, and (e) 80 W, respectively.

Table 2. The difference of the transmittance, the charge capacity and the coloration efficiency of the Ni-V-O film with respect to various of powers toward the Ni target.

Power (W)	10	20	30	50	80
$\Delta T(\%)$ at 600 nm	5.1	4.3	−0.9	−14.9	−35.2
Charge capacity (mC/cm ²)	47.88	33.10	14.28	57.90	101.35
Coloration efficiency (cm ² /C)	1.29	1.58	0.78	3.33	5.70

The ΔT values are very low at the samples of low power (<30 W) toward the Ni target of the Ni-O-V film as shown in Figure 5a–c. The ΔT decreases with the increase of Ni doping in the power region of 0–20 W. They are 5.1 and 4.3 at the power of 10 and 20 W, respectively. As the power increases to 30 W, its ΔT is −0.9%. The negative value of ΔT means the $T_{\text{reduction}}$ is higher than $T_{\text{oxidation}}$. This is because NiO is an oxidation electrochromic material and shows transparency at a reduction state [31] and it shares a reasonable portion in the Ni-V-O film.

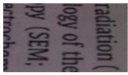
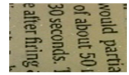
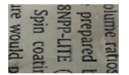
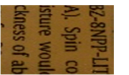
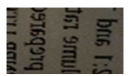
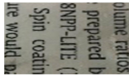
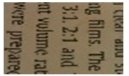
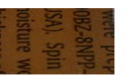
The transparency of the oxidation state decreases with the increase of the Ni doping of the Ni-V-O film as shown in the red circle line of Figure 5a–e. For the oxidation state, V₂O₅ is yellow color and the NiO is brown to intensify the coloration effect at the oxidation reaction.

As the reduction state of NiO is transparent, the transparency of the reduction state (green triangle) of the Ni-V-O films does not change obviously at the lower doping sample as shown in Figure 5a–d, while a degradation occurs at the sample of 80 W (Figure 5e). On account of the increase of the Ni doping, the ΔT decreases from 5.1 to −0.9% at the power range of 10–30 W. In the cases of sample 50 and 80 W, moreover, the ΔT values are down to −14.9% and −35.2%, respectively. The values become more negative due to the Ni-V-O thin film gradually being dominated by NiO compounds. As we discussed at Table 1, the atomic percentages of Ni and V are comparable and they are 18.83 and 19.30%, respectively, at the sample of 50 W. However, the atomic percentage of Ni comes to more than two times of V as the power is further increased to 80 W. Hence the electrochromism of the Ni-V-O film is dominated by V₂O₅ compounds at low Ni doping sample, while dominated by NiO compounds at high Ni doping.

The coloration efficiencies of the Ni-V-O thin films after various sputtering powers are also summarized in Table 2. The coloration efficiency of the Ni-V-O thin film is 1.29, 1.58, 0.78, 3.33, and 5.70 cm²/C for the sample with 10, 20, 30, 50, and 80 W, respectively, toward the Ni target. Higher power deposited Ni-V-O thin film shows higher coloration efficiency, as the CE value is 3.33 cm²/C at the sample of 50 W and 5.70 cm²/C at the sample of 80 W. This is because the sample of 80 W has a thicker thickness and its crystal structure is looser than the sample of lower power deposition. Therefore, it has a higher coloration rate.

Table 3 shows the photographs of colored and bleached states of the V₂O₅ thin film and the Ni-V-O thin film. For the Ni-V-O thin film, some critical conditions such as 10, 50, and 80 W were chosen to display the transparency difference.

Table 3. The photographs of colored and bleached states of the V₂O₅ thin film and the Ni-V-O thin film.

	V ₂ O ₅	Ni-V-O 10 W	Ni-V-O 50 W	Ni-V-O 80 W
Bleached				
Colored				

CV measurement was employed to investigate the effectiveness of the Ni-V-O thin films as ion storage layer of electrochromic devices, and the obtained results are displayed in Figure 6. Figure 6f shows the typical voltammogram of NiO. The voltammogram of V_2O_5 thin film with 10 W (Figure 6a) shows a similar loop to that of V_2O_5 film as shown in Figure 2. An oxidation peak was found at the potential between 0 and 1.3 V, and a reduction peak was found at the potential of -0.6 V. As the power is increased to 20 W (Figure 6b), the shape of the voltammogram loop of the Ni-V-O film transforms gradually and the oxidation and reduction peaks are not obvious. As the power increased to 30 W, the shape of the voltammogram loop as shown in Figure 6c depicts both oxidation and reduction peaks at potentials of 0.1 and -1.1 V, respectively. For the samples of 50 and 80 W, the shape of the voltammogram loops as presented in Figure 6d,e is similar to the shape of the voltammogram loop of pure NiO (Figure 6f). The atomic percentage of Ni is comparable to that of V at the sample of 50 W, and is larger than that of V at the sample of 80 W. This reveals the property of the Ni-V-O film is dominated by NiO compounds.

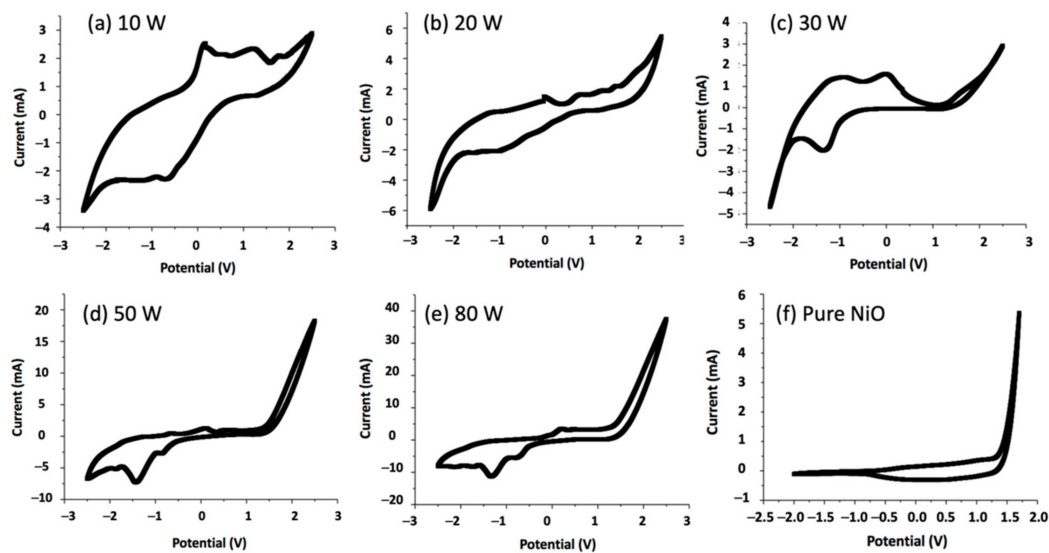


Figure 6. Cyclic voltammetry of the Ni-V-O thin films as ion storage layer of electrochromic device with various powers toward the Ni target, (a) 10 W, (b) 20 W, (c) 30 W, (d) 50 W, (e) 80 W, and (f) pure NiO, respectively.

The charge capacities of various power Ni-V-O film are summarized in Table 2. The charge capacity decreases from 47.88 to 14.28 mC/cm^2 at the power region of 10–30 W. The decrease is due to the transformation of the Ni-V-O film from the V_2O_5 dominate structure to a compactable mixing NiO and V_2O_5 . The charge capacity increases to 57.90 mC/cm^2 as the power is increased to 50 W, this is due to the NiO dominate gradually as indicated by the atomic percentage and the voltammogram. As the power is further increased to 80 W, the charge capacity increases to 101.35 mC/cm^2 , it shows a higher charge capacity the film with 80 W power toward the Ni target during deposition. The atomic percentage of Ni is 21.17% which is about two times of V (11.47%) at the sample of 80 W. The voltammogram of the CV curve of the 80 W sample becomes more similar to that of pure NiO. Additionally, we may say that the structure Ni-V-O film is NiO dominate. Due to the mixing of Ni and V of the Ni-V-O, the structure is looser than that of pure NiO film. This leads to a thicker thickness and high charge capacity of Ni-V-O film than that of dense pure NiO film. The current of CV of the 80 W sample as shown in Figure 6e is higher than that of pure NiO film as shown in Figure 6f.

4. Conclusions

In the research, the electrochromic properties of the V_2O_5 film and Ni-V-O film were presented. For the undoped V_2O_5 thin film, the transmittance difference at the wavelength of 600 nm increases from 1.8 to 25.6% as the deposition time of the V_2O_5 film increases from

1 to 3 h, indicating that the difference of transmittance between oxidation and reduction is increased as the thickness increased. For the Ni-V-O film, slight change of the film nature from pure V₂O₅ film occurred at the low doping power (<30 W) sample. The charge storage capacity decreases with the increase of Ni doping in this region. As the doping power is above 50 W, the amount of nickel in the film increases, the Ni-V-O films shows high transparency in the reduction reaction and also strengthens the coloring effect at the oxidation reaction. These effects are due to NiO structural domination of the Ni-V-O film. As the doping power was increased up to 80 W, better electrochromic property was obtained. The transmittance difference between colored and bleached states at a wavelength of 600 nm was 35.2% and the charge storage capacity increases to 101.35 mC/cm². Therefore, in comparison to pure V₂O₅ films, the Ni-V-O electrochromic films were proved to have certain advantages for the transmittance difference and charge storage capacity.

Author Contributions: Conceptualization, T.-C.L.; Formal analysis, B.-J.J.; Funding acquisition, T.-C.L.; Investigation, T.-C.L., B.-J.J. and W.-C.H.; Methodology, T.-C.L., B.-J.J. and W.-C.H.; Project administration, T.-C.L.; Resources, T.-C.L. and W.-C.H.; Software, T.-C.L. and W.-C.H.; Supervision, T.-C.L. and W.-C.H.; Validation, T.-C.L. and W.-C.H.; Visualization, T.-C.L. and W.-C.H.; Writing—Original draft, W.-C.H.; Writing—Review and editing, T.-C.L., B.-J.J. and W.-C.H. All authors have read and agreed to the published version of the manuscript.

Funding: This research is funded by the Ministry of Science and Technology (MOST) in Taiwan. The project number is MOST 107-2622-E-168-001-CC3.

Institutional Review Board Statement: Not applicable.

Informed Consent Statement: Not applicable.

Data Availability Statement: Data sharing not applicable.

Acknowledgments: The authors would also like to thank the financial support by the by the Green Energy Technology Research Center from The Featured Areas Research Center Program within the framework of the Higher Education Sprout Project by the Ministry of Education (MOE) in Taiwan.

Conflicts of Interest: The authors declare no conflict of interest.

References

1. Granqvist, C.G.; Green, S.; Niklasson, G.A.; Mlyuka, N.R.; Kræmer, S.V. Georén, Advances in chromogenic materials and devices. *Thin Solid Films* **2010**, *518*, 3046–3053. [[CrossRef](#)]
2. Wang, Y.; Runnerstrom, E.L.; Milliron, D.J. Switchable Materials for Smart Windows. *Annu. Rev. Chem. Biomol. Eng.* **2016**, *7*, 283–304. [[CrossRef](#)] [[PubMed](#)]
3. Granqvist, C.G. *Handbook of Inorganic Electrochromic Materials*, 1st ed.; Elsevier Science: Amsterdam, The Netherlands, 1995.
4. Granqvist, C.G.; Bayrak Pehlivan, İ.; Green, S.V.; Lansåker, P.C.; Niklasson, G.A. Oxide-Based Electrochromics: Advances in Materials and Devices. *MRS Online Proc. Libr.* **2011**, *1328*, 201. [[CrossRef](#)]
5. Benmoussa, M.; Outzourhit, A.; Bennouna, A.; Ameziane, E.L. Electrochromism in sputtered V₂O₅ thin films: Structural and optical studies. *Thin Solid Films* **2002**, *405*, 11–16. [[CrossRef](#)]
6. Semenenko, D.A.; Kozmenkova, A.Y.; Itkis, D.M.; Goodilin, E.A.; Kulova, T.L.; Skundin, A.M.; Tretyakov, Y.D. Growth of thin vanadia nanobelts with improved lithium storage capacity in hydrothermally aged vanadia gels. *CrystEngComm* **2012**, *14*, 1561–1567. [[CrossRef](#)]
7. Cogan, S.F.; Nguyen, N.M.; Perrotti, S.J.; Rauh, R.D. Optical properties of electrochromic vanadium pentoxide. *J. Appl. Phys.* **1989**, *66*, 1333–1337. [[CrossRef](#)]
8. Dickens, P.G.; Reynolds, G.J. Transport and equilibrium properties of some oxide insertion compound. *Solid State Ion.* **1981**, *5*, 331–334. [[CrossRef](#)]
9. Pan, A.; Zhang, J.G.; Nie, Z.; Cao, G.; Arey, B.W.; Li, G.; Liang, S.Q.; Liu, J. Facile synthesized nanorod structured vanadium pentoxide for high-rate lithium batteries. *J. Mater. Chem.* **2010**, *20*, 9193–9199. [[CrossRef](#)]
10. Rui, X.; Lu, Z.; Yin, Z.; Sim, D.H.; Xiao, N.; Lim, T.M.; Hng, H.H.; Zhang, H.; Yan, Q. Oriented molecular attachments through sol-gel chemistry for synthesis of ultrathin hydrated vanadium pentoxide nanosheets and their applications. *Small* **2013**, *9*, 716–721. [[CrossRef](#)]
11. Li, Y.H.; Lu, X.; Wang, R.; Yang, Y.; Duhm, S.; Fung, M.K. Cu-Doped nickel oxide prepared using a low-temperature combustion method as a hole-injection layer for high-performance OLEDs. *J. Mater. Chem.* **2017**, *C5*, 11751–11757. [[CrossRef](#)]
12. Kim, S.Y.; Yun, T.Y.; Yu, K.S.; Moon, H.C. Reliable, High-Performance Electrochromic Supercapacitors Based on Metal-Doped Nickel Oxide. *ACS Appl. Mater. Interfaces* **2020**, *12*, 51978–51986. [[CrossRef](#)]

13. Park, M.; Lim, Y.; Sung, Y.; Kwak, D.; Lee, J. Structure, morphology, and band gap of Ti-V-O mixed oxides processed by coprecipitation and calcination. *Acta Phys.* **2016**, *129*, 875–877. [[CrossRef](#)]
14. Ashrafi, M.A.; Ranjbar, M.; Kalhori, H.; Salamati, H. Pulsed laser deposition of Mo-V-O thin films for chromogenic applications. *Thin Solid Films* **2017**, *621*, 220–228. [[CrossRef](#)]
15. He, T.; Yao, J. Photochromism of molybdenum oxide. *J. Photochem. Photobiol. C Photochem. Rev.* **2003**, *4*, 125–143. [[CrossRef](#)]
16. Guinneton, F.; Sauques, L.; Valmalette, J.C.; Cros, F.; Gavarrri, J.R. Optimized infrared switching properties in thermochromic vanadium dioxide thin films: Role of deposition process and microstructure. *Thin Solid Films* **2004**, *446*, 287–295. [[CrossRef](#)]
17. Westphal, T.M.; Cholant, C.M.; Azevedo, C.F.; Moura, E.A.; da Silva, D.L.; Lemos, R.M.J.; Pawlicka, A.; Gündel, A.; Flores, W.H.; Avellaneda, C.O. Influence of the Nb₂O₅ doping on the electrochemical properties of V₂O₅ thin films. *J. Electro. Chem.* **2017**, *790*, 50–56. [[CrossRef](#)]
18. Xia, X.H.; Tu, J.P.; Zhang, J.; Wang, X.L.; Zhang, W.K.; Huang, H. Electrochromic properties of porous NiO thin films prepared by a chemical bath deposition. *Sol. Energy Mater. Sol. Cells* **2008**, *92*, 628–633. [[CrossRef](#)]
19. Kadam, L.D.; Patil, P.S. Studies on electrochromic properties of nickel oxide thin films prepared by spray pyrolysis technique. *Sol. Energy Mater. Sol. Cells* **2001**, *69*, 361–369. [[CrossRef](#)]
20. Purushothaman, K.K.; Joseph Antony, S.; Muralidharan, G. Optical, structural and electrochromic properties of nickel oxide films produced by sol-gel technique. *Solar Energy* **2011**, *85*, 978–984. [[CrossRef](#)]
21. Avendaño, E.; Azens, A.; Niklasson, G.A.; Granqvist, C.G. Nickel-oxide-based electrochromic films with optimized optical properties. *J. Solid State Electrochem.* **2003**, *8*, 37–39. [[CrossRef](#)]
22. Lampert, C.M.; Agrawal, A.; Baertlien, C.; Nagai, J. Durability evaluation of electrochromic devices—An industry perspective. *Sol. Energy Mater. Sol. Cells* **1999**, *56*, 449–463. [[CrossRef](#)]
23. Liu, H.; Yan, G.; Liu, F.; Zhong, Y.; Feng, B. Structural, electrochemical and optical properties of NiO_xH_y thin films prepared by electrochemical deposition. *J. Alloys Compd.* **2009**, *481*, 385–389. [[CrossRef](#)]
24. Kamal, H.; Elmaghraby, E.K.; Ali, S.A.; Abdel-Hady, K. The electrochromic behavior of nickel oxide films sprayed at different preparative conditions. *Thin Solid Films* **2005**, *483*, 330–339. [[CrossRef](#)]
25. Yaacob, M.H.; Yu, Y.; Latham, K.; Kalantar-zadeh, K.; Wlodarski, W. Optical Hydrogen Sensing Properties of Nanostructured Pd/MoO₃ Films. *Sens. Lett.* **2011**, *9*, 16–20. [[CrossRef](#)]
26. Lu, Y.R.; Hsu, H.H.; Chen, J.L.; Chang, H.W.; Chen, C.L.; Chou, W.C.; Dong, C.L. Atomic and electronic aspects of the coloration mechanism of gasochromic Pt/Mo-modified V₂O₅ smart films: An in situ X-ray spectroscopic study. *Phys. Chem. Chem. Phys.* **2016**, *18*, 5203–5210. [[CrossRef](#)]
27. Ranjbar, M.; Mahdavi, S.M.; Irajizad, A. Pulsed laser deposition of W-V-O composite films: Preparation, characterization and gasochromic studies. *Sol. Energy Mater. Sol. Cells* **2008**, *92*, 878–883. [[CrossRef](#)]
28. Deb, S.K. Opportunities and challenges in science and technology of WO₃ for electrochromic and related applications. *Sol. Energy Mater. Sol. Cells* **2008**, *92*, 245–258. [[CrossRef](#)]
29. Kalu, E.E.; Nwoga, T.T.; Srinivasan, V.; Weidner, J.W. Cyclic voltammetric studies of the effects of time and temperature on the capacitance of electrochemically deposited nickel hydroxide. *J. Power Sources* **2001**, *92*, 163–167. [[CrossRef](#)]
30. Özdemir, O.; Gökdemir, F.P.; Menda, U.D.; Kavak, P.; Saatci, A.E.; Kutlu, K. Nano-crystal V₂O₅/nH₂O sol-gel films made by dip coating. *AIP Conf. Proc.* **2012**, *147*, 233–240.
31. Purushothaman, K.K.; Muralidharan, G. Enhanced electrochromic performance of nanoporous NiO films. *Mater. Sci. Semicond. Process.* **2011**, *14*, 78–83. [[CrossRef](#)]